Renewable Energy 165 (2021) 14–24

Contents lists available at ScienceDirect

Renewable Energy

journal homepage: www.elsevier.com/locate/renene

The performance improvement of an indirect solar cooker using multi-walled carbon nanotube-oil nanofluid: An experimental study with thermodynamic analysis

Mohammad Hosseinzadeh [a, 1], Reza Sadeghirad [b, 1], Hosein Zamani [a, *], Ali Kianifar [b, **], Seyyed Mahdi Mirzababaee [a]

[a] Department of Food Industry Machineries, Research Institute of Food Science and Technology, Mashhad, Iran
[b] Department of Mechanical Engineering, Ferdowsi University of Mashhad, Mashhad, Iran

ARTICLE INFO

Article history:
Received 23 May 2020
Received in revised form
13 October 2020
Accepted 16 October 2020
Available online 23 October 2020

Keywords:
MWCNT
Solar collector
Cooking unit
Indirect solar cooker
Energy and exergy analyses

ABSTRACT

In this study, the effects of the volumetric flow rate of the nanofluid (250 ml/min, 350 ml/min, 450 ml/min and 550 ml/min) and the mass fraction of the nanoparticles (0 wt%, 0.2 wt% and 0.5 wt%) on the energy and exergy efficiencies of an indirect solar cooker with multi-walled carbon nanotube-oil (MWCNT-oil) nanofluid are investigated. Moreover, the performance of the solar collector and cooking unit, as the two main parts of the indirect solar cooker, is analyzed from the energy and exergy viewpoints. The results reveal that while increasing the volumetric flow rate of the nanofluid enhances the energy and exergy efficiencies of the solar collector, those of the cooking unit are maximized at the flow rate of 250 ml/min. Furthermore, using the nanofluid with a higher nanoparticles mass fraction leads the energy and exergy efficiencies of the solar collector and cooking unit to increase. Based on the results, the overall energy efficiency of the nanofluid-based solar cooker with 0.5 wt% is 20.08%, and the relative improvement of the overall exergy efficiency of the nanofluid-based solar cookers with 0.2 wt% and 0.5 wt% compared to that of the cooker with thermal oil is 37.30% and 65.87% respectively.

1. Introduction

One of the most reliable renewable energy sources is the sun, which provides the Earth with 3.85 million exajoules over a year [1]. Different systems, such as photovoltaic modules [2,3] and solar collectors [4,5], were manufactured so as to produce electrical and thermal energies using solar energy. Researchers have also endeavored to design an optimized solar system which makes cooking using solar energy possible. This system is called a solar cooker. One of the main challenges of solar cookers is that a user has to stay under the sun during the cooking process. This has affected the popularity of these systems in different countries especially in which the cost of fossil fuels is not high (such as Iran). To overcome this drawback, indirect solar cookers were proposed.

An indirect solar cooker is indeed a combination of a solar collector (located outdoors), cooking unit (situated indoors) and heat transfer medium [6]. In this system, having been heated in the solar collector, the heat transfer medium is conducted to the cooking unit. Water, thermal oil or nanofluid can be used as the heat transfer fluid in the structure of indirect solar cookers. Moreover, the type of solar collector can be concentrating type, flat plate or evacuated tube. As mentioned before, the main advantage of the indirect solar cooker is providing the indoor cooking possibility; however, it may be placed outdoors. This can be seen in the system including the solar collector integrated with heat pipes in which the heat pipes are inserted inside the cooking unit [7,8]. Generally, the indirect solar cookers can operate in either single-stage or double-stage modes [9,10]. In the single-stage mode, the heat transfer fluid is immediately led from the solar collector to the cooking unit, but in the other mode, the system operation comprises two phases, charging and discharging. During the charging phase, the gained energy by the heat transfer fluid is collected in a heat storage tank. This energy is then applied for cooking in the discharging phase.

Several studies in the literature investigated the performance of

* Corresponding author.
** Corresponding author.
E-mail addresses: mohammad.hz90@yahoo.com (M. Hosseinzadeh), h.zamani@rifst.ac.ir (H. Zamani), a-kiani@um.ac.ir (A. Kianifar).
[1] These authors have equal contribution in this article.

https://doi.org/10.1016/j.renene.2020.10.078

Nomenclature

A	Area (m^2)
c	Specific heat capacity (J kg^{-1} K^{-1})
$\dot{E}$	Power (W)
$\dot{E}x$	Exergy rate (W)
G	Solar radiation (W m^{-2})
h	Specific enthalpy (J kg^{-1})
m	Mass (kg)
$\dot{m}$	Mass flow rate (kg s^{-1})
P	Pressure (Pa)
s	Specific entropy (J kg^{-1} K^{-1})
T	Temperature (K)
t	Time (s)
u	Specific internal energy (J kg^{-1})

Greeks

η	Energy efficiency (%)
ε	Exergy efficiency (%)
ρ	Density (kg m^{-3})
φ	Nanoparticles volume fraction
ϕ	Non-flow exergy (J)

Subscripts

a	Aperture
amb	Ambient
ave	Average
bf	Base fluid
c	Coil
cu	Cooking unit
el	Electrical
f	Heat transfer fluid
fi	Final
i	Initial
in	Inlet
np	Nanoparticles
nf	Nanofluid
out	Outlet
ov	Overall
p	Pump
r	Receiver
sc	Solar collector
th	Thermal
w	Water

indirect solar cookers from different aspects. It should be noted that in the literature survey section, the research studies are categorized and presented based on the type of solar collector used in the structure of the indirect solar cooker. Haraksingh et al. [11] experimentally evaluated the performance of an indirect solar cooker including a double-glazed flat plate solar collector. In their thermosyphon system, the heat transfer fluid was coconut oil. They observed that when the cooking unit includes two pots with 2 L of water in each, the maximum oil temperature is 130 °C, whereas in the no-load condition, that of temperature in the cooking unit was reported to be 144 °C. Schwarzer and da Silva [12] presented an experimental procedure in order to examine different solar cookers. In addition, they experimentally studied the performance of an indirect solar cooker consisting of a flat plate solar collector. They achieved that in the average solar radiation of 900 W/m^2, the time taken to boil 8.5 kg of water with the initial temperature of 20 °C is nearly 60 min. Furthermore, about 32 kg of water can be boiled by the solar cooker over a day.

Esen [7] carried out experimental research to compare the effect of using different refrigerants in the heat pipes in an indirect solar cooker including an evacuated tube solar collector integrated with heat pipes. The investigated refrigerants were Freon 22 (R-22), Freon 134a (R-134a) and Freon 407C (R-407C). He concluded that the solar cooker with R-407C takes a lower time to cook different food namely rice, macaroni, potato, chicken and omelet. For example, the time required to cook 0.25 kg of rice in 0.4 kg of water in the system with R-407C was 50 min, while that of the cooker with R-22 and R-134a was reported to be 55 min and 63 min respectively. Sharma et al. [13] experimentally evaluated the performance of an indirect solar cooker with two evacuated tube solar collectors. In their study, the heat transfer fluid was water. Moreover, they used 45 kg of commercial erythritol as phase change material (PCM) in the cooking unit. They observed that even though cooking in the noon and evening are possible using the indirect solar cooker, the evening cooking takes a lower time. Their experimental results in the winter also show that the PCM did not melt during the experiment, so the solar cooker can be utilized for low-temperature cooking. In an experimental study, Farooqui [14] analyzed the efficiency of an indirect solar cooker from the energy and exergy viewpoints. The solar cooker included an evacuated tube and cooking unit, operating as a thermosyphon system. He found that the maximum energy efficiency of the solar cooker is in the range of 25–30%. In addition, its exergy efficiency peaks at 4.7%.

Mawire et al. [15] numerically investigated the charging phase of an indirect solar cooker which operated in the double-stage mode. They utilized a parabolic dish solar collector as well as a heat storage tank, containing oil (the heat transfer fluid) and pebbles, in the structure of the system. They achieved that rising the volumetric flow rate of oil from 12 ml/s to 18 ml/s causes both energy and exergy efficiencies of the system to increase. Furthermore, the effect of flow rate on exergy efficiency is higher than on energy efficiency. Kumaresan et al. [16] experimentally examined the discharge phase of an indirect solar cooker operating in the double-stage mode. However, they had charged the heat storage tank using a parabolic trough solar collector before the experiment. In their system, the heat storage tank included heat transfer fluid (Therminol 55 oil) and 126 PCM (D-Mannitol) balls. They concluded that the temperature of olive oil in the cooking unit rockets from 26 °C to its peak, 152 °C, within 15 min. They also reported that the cooking unit efficiency as well as the overall efficiency of the solar cooker in the discharge phase are 73.5% and 10.2% respectively.

Oommen and Jayaraman [17] experimentally evaluated the performance of an indirect solar cooker in which water is evaporated in a compound parabolic solar collector, and steam is then conducted to cooking unit. They observed that in the fabricated solar cooker, the time taken to cook 1 kg of rice in 1.5 L of water is 125 min. Saini et al. [18] experimentally studied the performance of an indirect solar cooker consisting of a parabolic trough solar collector. They used 3.5 kg of commercial Acetanilide as the PCM as well as water and engine oil as heat transfer fluids in their thermosyphon system. They found that in the no-load condition, the oil temperature is about 10–24 °C higher than that of water. In addition, using engine oil as the heat transfer fluid enhances the stored energy in the PCM by 19.45–30.38% in comparison with water. Therefore, the cooking time in the solar cooker with engine oil is lower than that of the system with water.

As reviewed above, the heat transfer fluid in the structure of indirect solar cookers was commonly oil or water. The use of nanofluids instead of conventional heat transfer fluids can be a useful method in order to enhance the performance of indirect solar cookers. Nevertheless, this matter was seldom examined in previous studies. In an experimental research effort, Abd-Elhady et al. [19] investigated the effect of using metallic wires and nanographene on the performance of an indirect solar cooker with parabolic trough solar collector in which an evacuated tube was situated at the focal line. In this study, the mass fraction of nanoparticles in the oil-based nanofluids was 3.4×10^{-4}%, 6.7×10^{-4}% and 1.0×10^{-3}%. They achieved that using the nanofluid with the nanoparticles mass fraction of 3.4×10^{-4}% slightly enhances the thermal performance of the indirect solar cooker. However, increasing the mass fraction of the nanoparticles has an adverse effect on the system performance. This is owing to the increase of the nanofluid viscosity, which influences the natural convection in the thermosyphon system.

The main goal of this study is to improve the performance of an indirect solar cooker using multi-walled carbon nanotube-oil (MWCNT-oil) nanofluid. The specific objectives of this research are expressed in the following:

- The experimental investigation of the efficiency of the solar collector and cooking unit as well as the overall efficiency of the indirect solar cooker from the energy and exergy viewpoints.
- The experimental evaluation of the effect of the volumetric flow rate of the nanofluid as well as the mass fraction of the nanoparticles on the performance of the indirect solar cooker.
- The comparison of the efficiency of the nanofluid-based indirect solar cooker with that of the system with thermal oil as the heat transfer fluid.

2. Experimental setup and nanofluid preparation

As shown in Fig. 1, the indirect solar cooker comprises two main sections being a parabolic dish solar collector and cooking unit. In the solar collector, a parabolic dish reflector, with an aperture diameter of 120 cm and depth of 20 cm, concentrates the solar radiation on an elliptically curved receiver. The focal length and concentration ratio of the reflector are 45 cm and 32.55 respectively. A view of the receiver inside is displayed in Fig. 2. According to the figure, the fabricated receiver consists of spiral blades, with a thickness of 1.5 mm and height of 12 mm. Moreover, the volume of the receiver is 400 ml. The heat transfer fluid is conducted into the receiver from a side with major diameter. The blades extend the heat transfer surface by leading the heat transfer fluid into a spiral passage before exiting the receiver from its center. Thus, the heat transfer fluid in the fabricated receiver absorbs higher thermal energy compared to in a conventional receiver. The cooking unit includes a helical coil which is welded around the cooking pot, and they are insulated by the K-Flex thermal insulation. Both of the helical coil and cooking vessel are made of copper. Furthermore, the internal diameter of the coil is 6 mm. A view of the cooking vessel along with the helical coil is shown in Fig. 3.

A schematic diagram of the experimental setup is illustrated in Fig. 4. As can be seen, the heat transfer fluid is conducted from a tank (located indoors) to the receiver using a pump. After being heated in the receiver, the heat transfer fluid is led to the cooking unit, where it conveys the thermal energy to the cooking vessel. In this study, the indirect solar cooker is utilized to boil 2 L of water. The experiments were carried out between 6 and July 24, 2019 at Research Institute of Food Science and Technology, Mashhad, Iran (Latitude: 36° and Longitude: 59°), commencing at 11:00, when the solar radiation intensity was high enough. The experimental data were recorded at intervals of 5 min until water started to boil. During the experiments, the flow rate of the heat transfer fluid was regulated and checked by a flow control valve as well as a beaker and timer. The ambient temperature was measured by a mercury thermometer which was situated near the experimental setup in the shade. In addition, solar radiation variations were monitored using a solar power meter (TES-1333, Taiwan). The water temperature as well as the temperature of the heat transfer fluid at the inlet and outlet of the receiver and helical coil were measured by means of K-type thermocouples. Moreover, a pressure transmitter (Atek, Turkey) was applied to measure the pressure of the heat transfer fluid.

In this research, the studied heat transfer fluids are Behran thermal oil and MWCNT-oil nanofluids with the nanoparticles mass

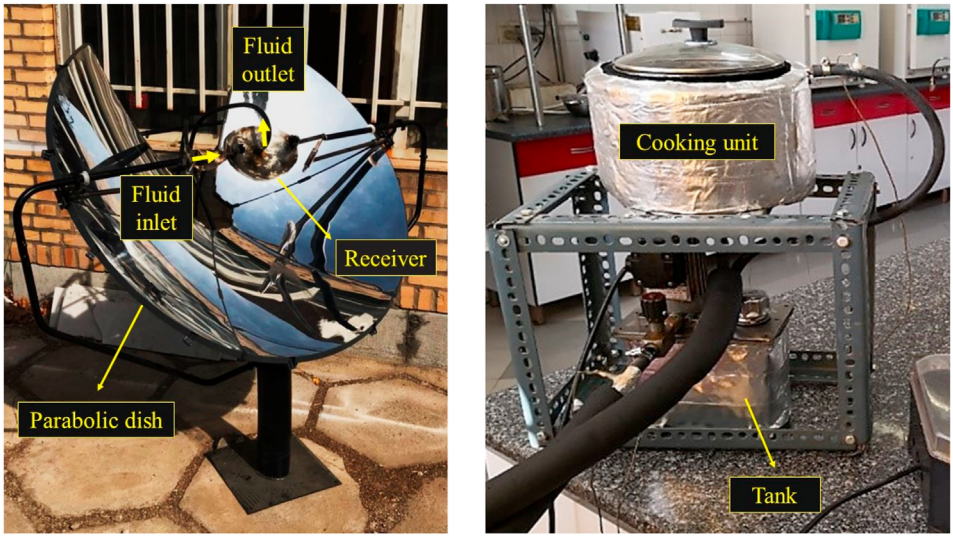

Fig. 1. A view of (a) solar collector and (b) cooking unit.

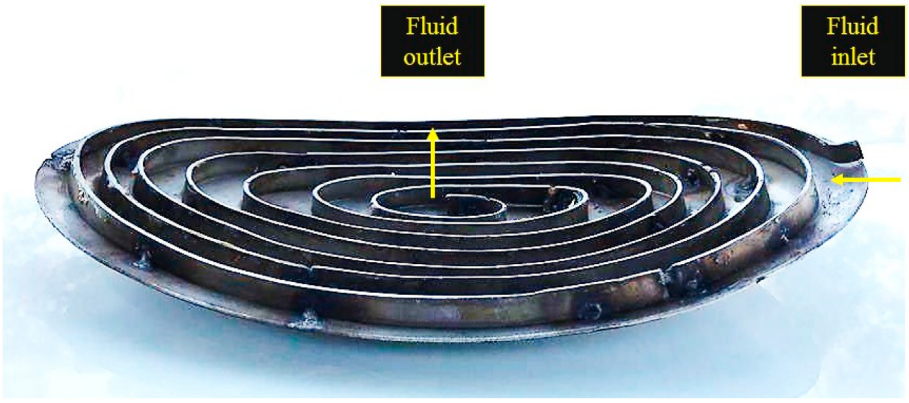

Fig. 2. A view of the receiver inside.

Fig. 3. A view of the cooking vessel along with the helical coil.

fraction of 0.2% and 0.5% (0.2 wt% and 0.5 wt%). The thermophysical properties of the thermal oil were presented in the previous studies [20,21]. Furthermore, the size and the thermophysical properties of MWCNT nanoparticles are reported in Table 1 [22,23]. The transmission electron microscope (TEM) image of the nanoparticles is also shown in Fig. 5. In order to prepare the nanofluids, a specific amount of the nanoparticles are initially added to the thermal oil and they are stirred manually. This is followed by stirring the suspension using a high-speed stirrer. The surfactant used in the preparation of the MWCNT-oil nanofluids is Gum Arabic [24]. To stabilize the mixture, this is then exposed to ultrasonication with a constant temperature of 50 °C in an ultrasound vibrator (Elma, Elmasonic, Germany). It should be mentioned that the ultrasonication process is performed in four time periods of 30 min. For instance, a view of the prepared MWCNT-oil nanofluid with 0.2 wt% is displayed in Fig. 6.

3. Thermodynamic analysis

In this section, the energy and exergy analyses are presented so as to investigate the performance of the solar collector and cooking unit, as the two main sections of the indirect solar cooker. Moreover, the overall performance of the indirect solar cooker is

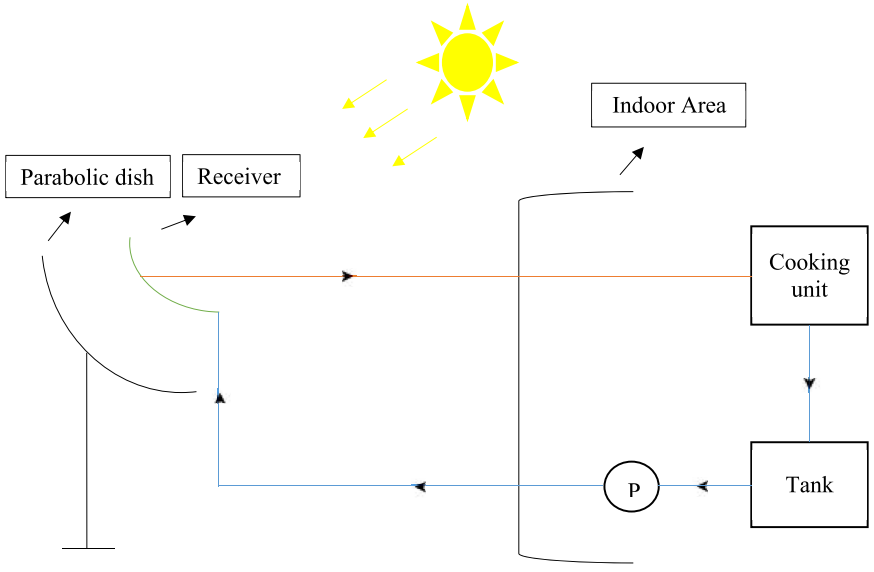

Fig. 4. The schematic diagram of the experimental setup.

Table 1
The size and thermophysical properties of MWCNT nanoparticles [22,23].

Particle size (nm)	Density (kg m^{-3})	Heat capacity (J kg^{-1} K^{-1})	Thermal conductivity (W m^{-1} K^{-1})
10–20	2100	735	1500–3000

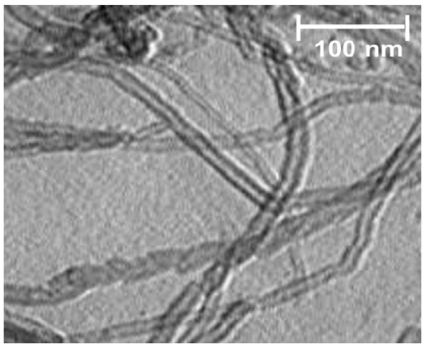

Fig. 5. TEM image of MWCNT nanoparticles.

Fig. 6. A view of the prepared MWCNT-oil nanofluid with 0.2 wt%.

evaluated from the energy and exergy viewpoints.

3.1. Solar collector

By considering the solar collector as a control volume, the rate of input solar energy is calculated by the following equation:

$$\dot{E}_{sc,in} = GA_a \tag{1}$$

where G is the rate of total solar radiation, and A_a refers to the aperture area of the solar concentrator, which is 0.94 m^2. The output thermal power of the solar collector is expressed as:

$$\dot{E}_{sc,out} = \dot{m}_f c_f (T_{r,out} - T_{r,in}) \tag{2}$$

In the above equation, $\dot{m}_f$ represents the mass flow rate of heat transfer fluid. In addition, c_f is the specific heat capacity of the heat transfer fluid. $T_{r,in}$ and $T_{r,out}$ refer to the temperature of the heat transfer fluid at the inlet and outlet of the receiver respectively. If the heat transfer fluid of the indirect solar cooker is nanofluid, the specific heat capacity can be obtained as follows [25]:

$$c_{nf} = \frac{\varphi(\rho_{np} c_{np}) + (1-\varphi)(\rho_{bf} c_{bf})}{\rho_{nf}} \tag{3}$$

in which φ and ρ_{nf} indicate the volume fraction of nanoparticles and the density of the nanofluid in order, which are calculated using the following equations [25]:

$$\varphi = \frac{m_{np}/\rho_{np}}{m_{np}/\rho_{np} + m_{bf}/\rho_{bf}} \tag{4}$$

$$\rho_{nf} = \varphi\rho_{np} + (1-\varphi)\rho_{bf} \tag{5}$$

Using Eqs. (1) and (2), the instantaneous energy efficiency of the solar collector is obtained as follows:

$$\eta_{sc} = \frac{\dot{E}_{sc,out}}{\dot{E}_{sc,in}} = \frac{\dot{m}_f c_f (T_{r,out} - T_{r,in})}{GA_a} \tag{6}$$

The exergy rate of the input solar energy can be calculated as [26,27]:

$$\dot{E}x_{sc,in} = GA_a[1 - \frac{4T_{amb}}{3T_{sun}} + \frac{1}{3}(\frac{T_{amb}}{T_{sun}})^4] \tag{7}$$

In the above equation, T_{amb} refers to the ambient temperature, and T_{sun} is the temperature of the sun as a black body (being 5800 K) [28]. The output thermal exergy rate of the solar collector is obtained by the difference between the flow (stream) exergy at the inlet and outlet of the receiver, which is expressed as [25,29]:

$$\dot{E}x_{sc,out} = \dot{E}x_{r,out} - \dot{E}x_{r,in} = \dot{m}_f[(h_{r,out} - h_{r,in}) - T_{amb}(s_{r,out} - s_{r,in})] \rightarrow$$
$$\dot{E}x_{sc,out} = \dot{m}_f c_f[(T_{r,out} - T_{r,in}) - T_{amb}\ln(\frac{T_{r,out}}{T_{r,in}})] \tag{8}$$

where h_r and s_r represent the specific enthalpy and entropy of the heat transfer fluid respectively. Based on Eqs. (7) and (8), the instantaneous exergy efficiency of the solar collector is calculated by the following equation:

$$\varepsilon_{sc} = \frac{\dot{E}x_{sc,out}}{\dot{E}x_{sc,in}} = \frac{\dot{m}_f c_f[(T_{r,out} - T_{r,in}) - T_{amb}\ln(\frac{T_{r,out}}{T_{r,in}})]}{GA_a[1 - \frac{4T_{amb}}{3T_{sun}} + \frac{1}{3}(\frac{T_{amb}}{T_{sun}})^4]} \tag{9}$$

3.2. Cooking unit

By considering the cooking unit as a control volume, the input thermal power which is provided by the helical coil is obtained as follows:

$$\dot{E}_{cu,in} = \dot{m}_f c_f (T_{c,in} - T_{c,out}) \tag{10}$$

in which $T_{c,in}$ and $T_{c,out}$ are the temperature of the heat transfer fluid at the inlet and outlet of the helical coil in order. The average output thermal power of the cooking unit is expressed as the average rate of thermal energy which water absorbs during a time interval. This is calculated using the following equation [16,27]:

$$\dot{E}_{cu,out,ave} = \frac{m_w c_w (T_{w,fi} - T_{w,i})}{\Delta t} \tag{11}$$

where m_w indicates the mass of water, and c_w is the specific heat

capacity of water. Moreover, $T_{w,i}$ and $T_{w,fi}$ refer to the water temperature at the beginning and end of the time interval respectively. Using Eqs. (10) and (11), the average energy efficiency of the cooking unit during the time interval is expressed as [10]:

$$\eta_{cu} = \frac{\dot{E}_{cu,out,ave}}{\dot{E}_{cu,in,ave}} \tag{12}$$

In the above equation, $\dot{E}_{cu,in,ave}$ is the average input thermal power of the cooking unit during the time interval. Similar to Eq. (8), the input thermal exergy rate of the cooking unit is calculated by the difference between the flow exergy at the inlet and outlet of the helical coil:

$$\dot{E}x_{cu,in} = \dot{m}_f c_f[(T_{c,in} - T_{c,out}) - T_{amb}\ln(\frac{T_{c,in}}{T_{c,out}})] \tag{13}$$

The exergy change of water as well as the average rate of the output thermal exergy of the cooking unit over the time interval are calculated by the following equations [30,31]:

$$\Delta\phi_w = \phi_{w,fi} - \phi_{w,i} = m_w[(u_{w,fi} - u_{w,i}) - T_{amb}(s_{w,fi} - s_{w,i})] \rightarrow$$
$$\Delta\phi_w = m_w c_w[(T_{w,fi} - T_{w,i}) - T_{amb}\ln(\frac{T_{w,fi}}{T_{w,i}})] \tag{14}$$

$$\dot{E}x_{cu,out,ave} = \frac{\Delta\phi_w}{\Delta t} = \frac{m_w c_w[(T_{w,fi} - T_{w,i}) - T_{amb}\ln(\frac{T_{w,fi}}{T_{w,i}})]}{\Delta t} \tag{15}$$

in which ϕ_w and u_w represent the exergy and specific internal energy of water respectively. Based on Eqs. (13) and (15), the average exergy efficiency of the cooking unit during the time interval is obtained as follows:

$$\varepsilon_{cu} = \frac{\dot{E}x_{cu,out,ave}}{\dot{E}x_{cu,in,ave}} \tag{16}$$

In the above equation, $\dot{E}x_{cu,in,ave}$ is the average rate of the input thermal exergy of the cooking unit during the time interval.

3.3. The overall performance of indirect solar cooker

The electrical power consumed by the pump so as to circulate the heat transfer fluid in the system can be calculated as [32]:

$$\dot{E}_p = \frac{\dot{m}_f \Delta P}{\rho_f \eta_p} \tag{17}$$

where ΔP indicates the pressure drop in the system. Furthermore, η_p is the pump efficiency.

The overall energy efficiency of the indirect solar cooker depends on the output thermal power of the cooking unit and input solar power. It should be noted that in order to calculate the cooker efficiency, the consumed pumping power is subtracted from the output thermal power of the solar cooker. For this purpose, the electrical pumping power is initially converted to an equivalent thermal power by dividing the pumping power to a factor of η_{el} which is considered to be 0.33 [33]. Thus, the overall energy efficiency of the indirect solar cooker is calculated using the following equation:

$$\eta_{ov} = \frac{\dot{E}_{cu,out,ave} - \frac{\dot{E}_p}{\eta_{el}}}{A_a \int_{t_1}^{t_2} G(t)dt} = \frac{\dot{E}_{cu,out,ave} - \frac{\dot{E}_p}{\eta_{el}}}{\dot{E}_{sc,in,ave}} \tag{18}$$

In the above equation, $\dot{E}_{sc,in,ave}$ is the average rate of the input solar energy over the time interval. Since electrical energy is equivalent to available work, the pumping exergy rate is equal to the pumping power [25]. Consequently, the overall exergy efficiency of the indirect solar cooker is expressed as:

$$\varepsilon_{ov} = \frac{\dot{E}x_{cu,out,ave} - \dot{E}_p}{\dot{E}x_{sc,in,ave}} \tag{19}$$

in which $\dot{E}x_{sc,in,ave}$ refers to the average exergy rate of the input solar energy during the time interval.

4. Uncertainty analysis

In an experimental study, the uncertainty analysis is implemented to investigate the reliability of the results. For a measured parameter, the total uncertainty is calculated using the following equation [6,34]:

$$\delta v = \sqrt{(\delta v_{equ})^2 + (\delta v_{rep})^2} \tag{20}$$

where δv_{equ} represents the equipment uncertainty, depending upon the accuracy of the equipment. In addition, δv_{rep} is the repetition uncertainty, which demonstrates the repeatability of the experimental data. If F is a function of independent linear parameters, $F = F(v_1, v_2, ..., v_n)$, the uncertainty of this function can be obtained as follows [35]:

$$\delta F = \sqrt{(\frac{\partial F}{\partial v_1}\delta v_1)^2 + (\frac{\partial F}{\partial v_2}\delta v_2)^2 + ... + (\frac{\partial F}{\partial v_n}\delta v_n)^2} \tag{21}$$

The accuracy of the equipment as well as the total uncertainty of the parameters measured during the experiments are presented in Table 2. The analyses also reveal that the maximum uncertainty of all parameters is less than 4%. This demonstrates the reliability of the experimental results.

5. Results and discussion

In this research, the effects of the volumetric flow rate of MWCNT-oil nanofluid as well as the mass fraction of nanoparticles in the nanofluid on the energy and exergy efficiencies of the indirect solar cooker are presented.

5.1. Effect of volumetric flow rate

In this section, the indirect solar cooker is experimentally examined so as to study how the variation of the volumetric flow rate of MWCNT-oil nanofluid with 0.2 wt% can affect the performance of the solar collector and cooking unit separately. Furthermore, its effect on the overall efficiency of the solar cooker is evaluated. The studied flow rates are 250 ml/min, 350 ml/min, 450 ml/min and 550 ml/min. The experiments regarding each flow rate were accomplished in separate days between 6 and July 18, 2019. For instance, Fig. 7 shows the variation of the solar radiation and ambient temperature during the experiment in which the volumetric flow rate of the nanofluid was 250 ml/min. The experiment was performed on July 6, 2019. According to the figure, the

Table 2
The total uncertainty of the measured parameters during the experiments.

Measured parameter	Measuring equipment	Equipment accuracy	Uncertainty
Solar radiation	Solar power meter (TES-1333, Taiwan)	±10.0 W/m^2 or ±5% (additional ±0.38 W/m^2/°C for T ≥ 25 °C)	±3.39 W/m^2
Ambient temperature	Mercury thermometer	±0.5 °C	±0.54 °C
Fluid inlet temperature (receiver)	K-type thermocouple (Wire type)	±1.5 °C or ±0.75% (0 °C ≤ T ≤ 200 °C)	±0.78 °C
Fluid outlet temperature (receiver)	K-type thermocouple (Wire type)	±1.5 °C or ±0.75% (0 °C ≤ T ≤ 200 °C)	±0.88 °C
Fluid inlet temperature (helical coil)	K-type thermocouple (Wire type)	±1.5 °C or ±0.75% (0 °C ≤ T ≤ 200 °C)	±0.73 °C
Fluid outlet temperature (helical coil)	K-type thermocouple (Wire type)	±1.5 °C or ±0.75% (0 °C ≤ T ≤ 200 °C)	±0.74 °C
Water temperature	K-type thermocouple (Probe type)	±(0.5 °C + 0.3% of m.v.) (-40 °C ≤ T ≤ 900 °C)	±0.46 °C

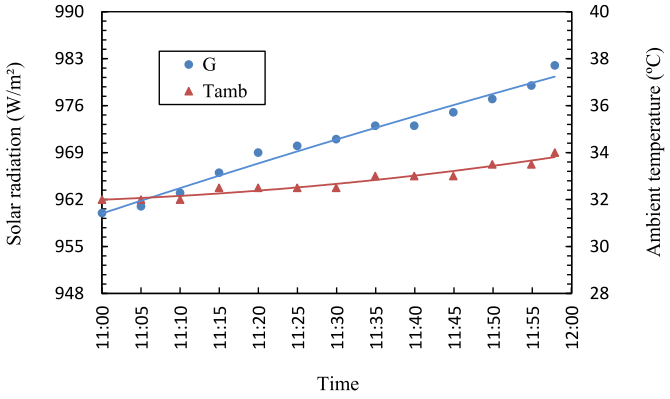

Fig. 7. The variation of solar radiation and ambient temperature in the experiment with the volumetric flow rate of 250 ml/min (date: July 6, 2019).

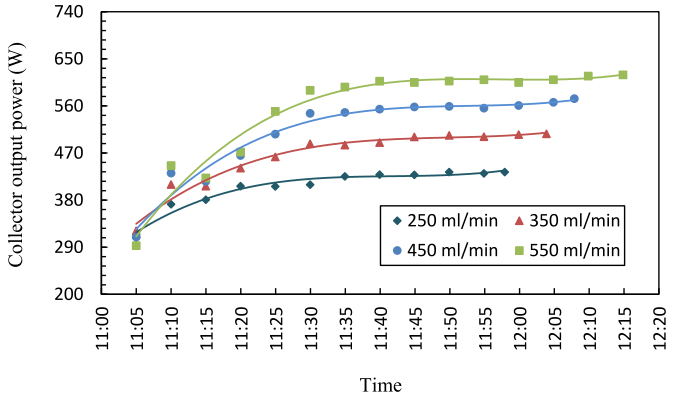

Fig. 8. The variation of the output thermal power of the solar collector for different flow rates.

Table 3
The average solar radiation and ambient temperature for different experiment (each experiment was carried out in a typical day between 6 and July 18, 2019).

Parameter	Volumetric flow rate (ml/min)			
	250	350	450	550
Solar radiation (W/m^2)	970.69	968.64	971.33	973.44
Ambient temperature (◦C)	32.77	31.96	32.17	33.19

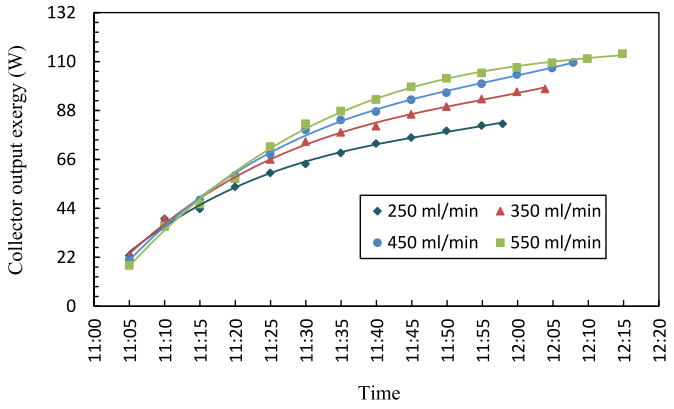

Fig. 9. The variation of the output thermal exergy rate of the solar collector for different flow rates.

weather parameters saw a slight variation during the test, with an increase of 22 W/m^2 and 2 °C for the solar radiation and ambient temperature respectively. Moreover, the average weather parameters for the different experiments are listed in Table 3. The table demonstrates that the experiments were conducted in rather similar weather conditions.

5.1.1. Analysis of solar collector

The variation of the output thermal power of the solar collector for the four volumetric flow rates is displayed in Fig. 8. In a constant flow rate, using Eq. (2), the output thermal power of the solar collector initially witnesses a sharp rise owing to the increase of fluid temperature difference between the inlet and outlet of the receiver. It then levels off over the rest of the test period. In the case of the volumetric flow rate of 250 ml/min, the collector output thermal power surges from 307.83 W (at 11:05) to 425.25 W (at 11:35), followed by a slight growth until it peaks at 433.63 W. In a low flow rate, the receiver temperature and consequently heat loss from the receiver are more than those of the collector with a higher flow rate. Hence as shown in Fig. 8, the output thermal power of the solar collector enhances by increasing the flow rate.

Fig. 9 illustrates the variation of the output thermal exergy rate of the solar collector for different cases. In a constant flow rate, not only $(T_{r,out} - T_{r,in})$ but also $(\frac{T_{r,out}}{T_{r,in}})$ rises during the test period; the latter increase, nevertheless, has an adverse effect on the collector output thermal exergy. Using Eq. (8), the results demonstrate that the output thermal exergy rate of the solar collector improves over the test period. In the experiment with the volumetric flow rate of 250 ml/min, the enhancement of the output thermal exergy rate is 59.27 W. Based on Fig. 9, similar to the output thermal power, the output thermal exergy rate of the solar collector goes up by rising the flow rate. The analyses show that the average output thermal exergy rate of the solar collector is 61.96 W, 71.47 W, 78.05 W and 82.67 W for the volumetric flow rates of 250 ml/min, 350 ml/min, 450 ml/min and 550 ml/min respectively. These values are noticeably lower in comparison with the corresponding output thermal powers, which proves the low quality of the output thermal power in the solar collector.

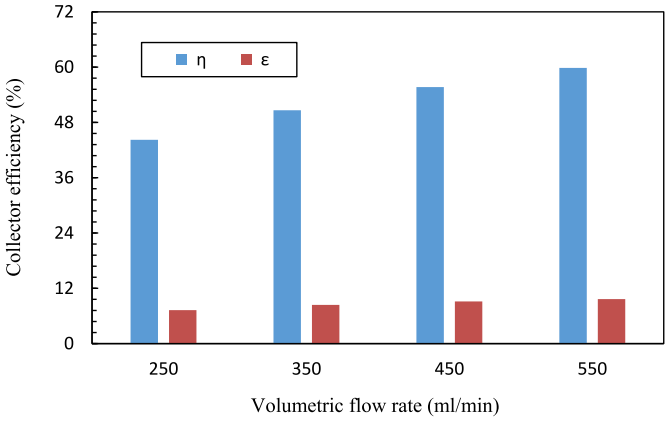

Fig. 10. The average energy and exergy efficiencies of the solar collector for different flow rates.

Fig. 10 provides information regarding the average energy and exergy efficiencies of the solar collector for the four volumetric flow rates. As mentioned before, the experiments were performed in a similar weather condition. Moreover, the output thermal power and output thermal exergy rate of the solar collector enhance by increasing the flow rate. Thus, according to Eqs. (6) and (9), rising the volumetric flow rate from 250 ml/min to 550 ml/min improve the energy and exergy efficiencies of the solar collector by 15.60 and 2.39% points in order.

5.1.2. Analysis of cooking unit and indirect solar cooker

The variation of water temperature in the cooking unit for the four cases is shown in Fig. 11 (a). During the experiments, the water temperature was recorded until it reached the boiling point. The data indicate that the time required to boil 2 L of water in the test with the volumetric flow rate of 250 ml/min is 58 min, and rising the flow rate increases the time, being 64 min, 68 min and 75 min for the flow rates of 350 ml/min, 450 ml/min and 550 ml/min respectively. Hence, increasing the flow rate from 250 ml/min to 550 ml/min raises the time taken to boil water by 17 min (29.31%). This is attributed to the reduction of the absorbed energy by water. To investigate this matter, the variation of the output thermal power of the cooking unit for the four volumetric flow rates is illustrated in Fig. 11 (b). Based on Eqs. (11) and (15), in the cooking unit, the energy and exergy outputs are obtained over a time interval of 5 min, represented at the end of the time interval in the figures. For instance, the maximum output thermal power of 228.73 W which is displayed for the case with the flow rate of 250 ml/min at 11:15 in Fig. 11 (b) is indeed the average output thermal power of the cooking unit from 11:10 to 11:15. In a constant flow rate, using Eq. (11), the output thermal power of the cooking unit initially rises to reach its peak. The variation of water temperature difference during the time intervals demonstrates that the output thermal power then experiences a declining trend until the end of the experiment. As mentioned before, in the indirect solar cooker, the nanofluid is conducted to the cooking unit after it has absorbed thermal energy from the receiver. Therefore, in a low flow rate, the nanofluid temperature at the inlet of the helical coil is more than that of the solar cooker with a higher flow rate, which causes the output thermal power of the cooking unit to grow. According to the results, the average output thermal power of the cooking unit is 145.66 W, 134.93 W, 125.95 W and 113.46 W for the volumetric flow rates of 250 ml/min, 350 ml/min, 450 ml/min and 550 ml/min in order. Thus, using the flow rate of 250 ml/min in preference to 550 ml/min in the indirect solar cooker enhances the average output thermal power of the cooking unit by 32.20 W (28.38%).

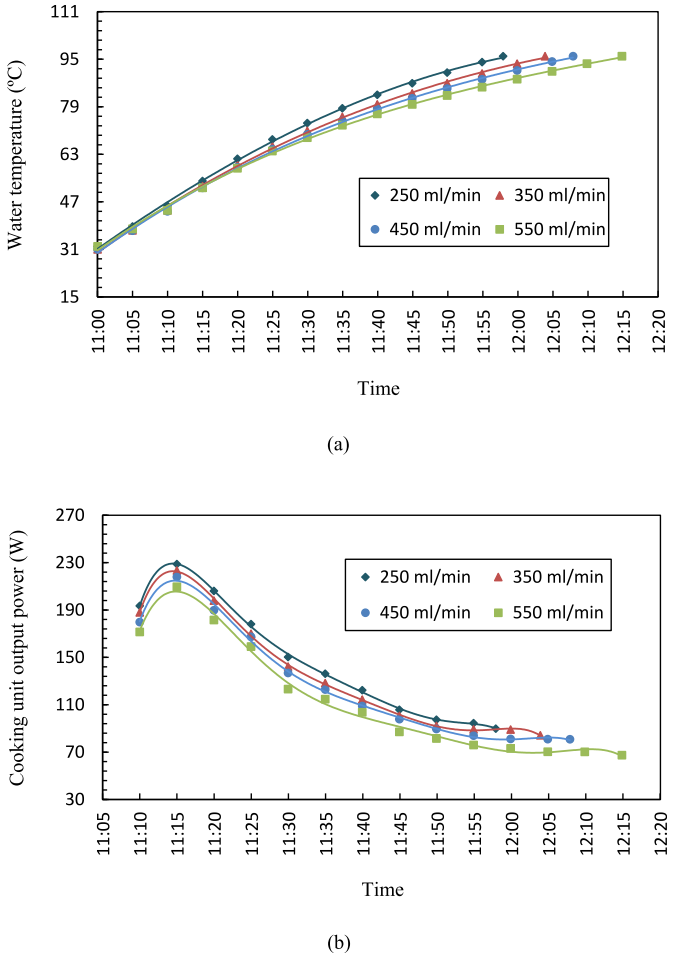

Fig. 11. The variation of (a) water temperature in the cooking unit and (b) output thermal power of the cooking unit for different flow rates.

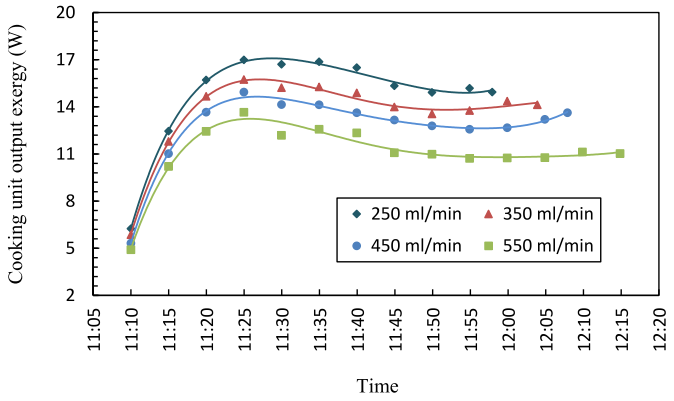

Fig. 12. The variation of the output thermal exergy rate of the cooking unit for different flow rates.

Fig. 12 indicates the variation of the output thermal exergy rate of the cooking unit for different cases. The experimental data represent that apart from an initial growth over the first three intervals, both $(T_{w,fi} - T_{w,i})$ and $(\frac{T_{w,fi}}{T_{w,i}})$ values decrease over the rest of test period in the experiments with a constant flow rate. Furthermore, these values diminish by rising the flow rate. Using Eq. (15),

Table 4
The average energy and exergy efficiencies of the cooking unit and indirect solar cooker for different flow rates.

System	Parameter	Volumetric flow rate (ml/min)			
		250	350	450	550
Cooking unit	Energy efficiency (%)	61.58	54.72	50.34	43.93
	Exergy efficiency (%)	40.74	36.35	34.06	29.52
Solar cooker	Overall energy efficiency (%)	15.93	14.79	13.78	12.39
	Overall exergy efficiency (%)	1.73	1.60	1.49	1.29

the average output thermal exergy rate of the cooking unit in the case with the volumetric flow rate of 250 ml/min is 14.71 W, being about 1.11 W, 2.03 W and 3.66 W higher than that of the systems with the volumetric flow rates of 350 ml/min, 450 ml/min and 550 ml/min respectively. Moreover, the comparison of the output thermal exergy rate of the cooking unit with its output thermal power implies that the quality of the output thermal power in the cooking unit is low. This is also inferior to the quality of the output thermal power in the solar collector.

The average energy and exergy efficiencies of the cooking unit and indirect solar cooker for the four volumetric flow rates are presented in Table 4. The results reveal that the energy and exergy efficiencies of the cooking unit decline about 17.65 and 11.22% points by increasing the volumetric flow rate from 250 ml/min to 550 ml/min. Based on Eq. (17), the consumed power to circulate the nanofluid in the indirect solar cooker is approximately negligible compared to the output thermal power of the cooking unit for the different cases. Table 4 also indicates that in the case with the flow rate of 250 ml/min, the overall energy and exergy efficiencies of the indirect solar cooker are 15.93% and 1.73%, which are by 3.54 and 0.44% points higher than those of the cooker with the volumetric flow rate of 550 ml/min respectively.

5.2. Effect of nanoparticles mass fraction

In this section, the effects of using MWCNT-oil nanofluids with 0.2 wt% and 0.5 wt% as the heat transfer fluids on the performance of the solar collector and cooking unit as well as the overall performance of the indirect solar cooker are evaluated from the energy and exergy viewpoints. Moreover, the nanofluid-based indirect solar cookers are compared with the cooker with thermal oil. It should be mentioned that the results presented in section 5.1 demonstrate that the solar cooker with the volumetric flow rate of 250 ml/min has higher overall energy and exergy efficiencies in comparison with the other cases. Therefore, this flow rate was utilized in the experiments. The average solar radiation during the experiments was 970.69 W/m^2, 964.91 W/m^2 and 969.19 W/m^2 for the test with the heat transfer fluids of MWCNT-oil nanofluids with 0.2 wt% and 0.5 wt%, and thermal oil respectively. In addition, the corresponding values for the ambient temperature were 32.77 °C, 32.27 °C and 34.94 °C in order. These indicate that the experiments were performed in rather similar weather conditions.

5.2.1. Analysis of solar collector

Fig. 13 (a) and (b) illustrate the variations of the energy and exergy efficiencies of the solar collector for the three heat transfer fluids. Since increasing the mass fraction of the nanoparticles improves the heat transfer characteristics, the output thermal power and consequently the energy efficiency of the solar collector rise. According to Fig. 13 (a), the average energy efficiency of the solar collector is 37.46%, 44.24% and 48.05% for the heat transfer fluid of thermal oil and MWCNT-oil nanofluids with 0.2 wt% and 0.5 wt% respectively. The results also indicate that both $(T_{r,out} - T_{r,in})$ and

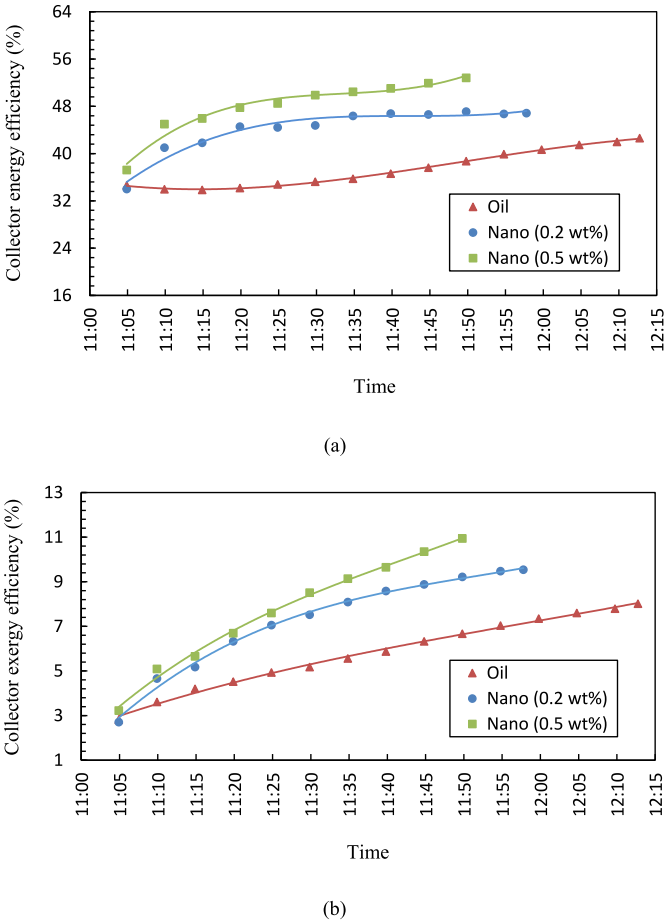

Fig. 13. The variation of (a) the energy efficiency and (b) exergy efficiency of the solar collector for different heat transfer fluids.

$(\frac{T_{r,out}}{T_{r,in}})$ grow by rising the mass fraction of the nanoparticles. Based on Eq. (9), the increase of nanoparticles mass fraction also improves the output thermal exergy rate and thus the exergy efficiency of the solar collector. As shown in Fig. 13 (b), the use of the nanofluids with 0.2 wt% and 0.5 wt% raises the exergy efficiency of the solar collector by 1.44 and 1.85% points compared to the system with thermal oil. Fig. 13 (a) and (b) also represent that the exergy efficiency of the solar collector is considerably lower than its energy

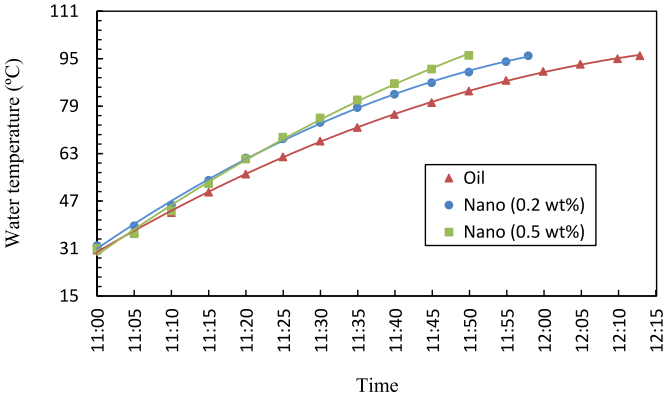

Fig. 14. The variation of water temperature in the cooking unit for different heat transfer fluids.

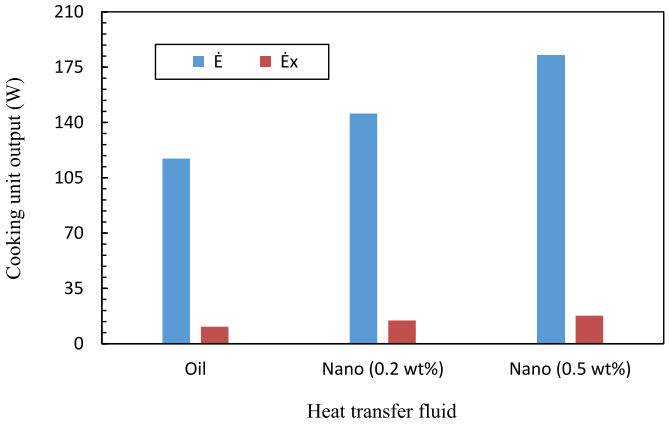

Fig. 15. The average output thermal power and exergy rate of the cooking unit for different heat transfer fluids.

efficiency because of the low quality of the output thermal power in the solar collector.

5.2.2. Analysis of cooking unit and indirect solar cooker

Fig. 14 displays the variation of water temperature for the three cases. As mentioned before, the volumetric flow rate of the heat transfer fluids was 250 ml/min in the experiments. According to experimental data, 73 min is required to boil 2 L of water in the indirect solar cooker with thermal oil. However, the use of MWCNT-oil nanofluids with 0.2 wt% and 0.5 wt% reduces the time to 58 min and 50 min respectively. Therefore, the use of the latter nanofluid in preference to thermal oil decreases the time taken to boil water about 23 min (31.51%).

The average output thermal power and exergy rate of the cooking unit for the three heat transfer fluids are shown in Fig. 15. The fluid temperature at the inlet of the helical coil as well as the heat transfer characteristics improve by rising the mass fraction of the nanoparticles, which cause the output thermal power of the cooking unit to increase. The average output thermal power of the cooking unit for the nanofluid with 0.5 wt% is 182.64 W. This is about 36.98 W (25.39%) and 65.52 W (55.95%) higher than that of the nanofluid with 0.2 wt% and thermal oil respectively. As seen in Fig. 15, increasing the nanoparticles mass fraction also enhances the output thermal exergy rate of the cooking unit, being 10.71 W, 14.71 W and 17.71 W for the heat transfer fluid of thermal oil and MWCNT-oil nanofluids with 0.2 wt% and 0.5 wt% in order.

By considering the characteristics of the indirect solar cookers, the energy and exergy efficiencies of the cooking unit and indirect solar cooker in the present study are compared to those in previous researches. Based on Table 5, few studies investigated the efficiency of the cooking unit and indirect solar cooker based on both energy and exergy viewpoints. The results of this study demonstrate that using MWCNT-oil nanofluid with 0.5 wt% instead of thermal oil raises the energy and exergy efficiencies of the cooking unit by 12.56 and 9.13% points in order. It should be noted that during the experiments, the maximum pumping power is about 0.27 W, which is negligible compared to the output thermal power of the cooking unit. Thus, the pumping power has been ignored in the analyses. Moreover, the nanofluid-based indirect solar cookers have higher overall energy and exergy efficiencies in comparison with the cooker with thermal oil due to the superior output thermal power and output thermal exergy rate of the cooking unit. Table 5 indicates that the overall energy efficiency of the solar cooker with thermal oil and the nanofluids with 0.2 wt% and 0.5 wt% is 12.85%, 15.93% and 20.08% respectively. Furthermore, the relative enhancement of the overall exergy efficiency of the nanofluid-based solar cookers with 0.2 wt% and 0.5 wt% compared to that of the cooker with thermal oil is 37.30% and 65.87% in order.

6. Conclusions

In this study, the overall performance of a nanofluid-based indirect solar cooker is analyzed from the energy and exergy viewpoints. Moreover, the efficiencies of the solar collector and cooking unit, as the two main parts of the indirect solar cooker, are evaluated. The investigated parameters in this research are the volumetric flow rate of MWCNT-oil nanofluid (ranging from 250 ml/min to 550 ml/min) and the nanoparticles mass fraction in the nanofluid (in the range of 0 wt% to 0.5 wt%). The main conclusions are summarized in the following:

- Increasing the volumetric flow rate of MWCNT-oil nanofluid from 250 ml/min to 550 ml/min improves the performance of the solar collector based on both energy and exergy viewpoints. In the case of energy and exergy efficiencies, the corresponding enhancements are 15.60 and 2.39% points respectively.
- Contrary to the solar collector, among the studied flow rates, the maximum energy and exergy outputs of the cooking unit as well as the maximum overall energy and exergy efficiencies of the indirect solar cooker are achieved in the system with the volumetric flow rate of 250 ml/min, in which the output thermal power and output thermal exergy rate of the cooking unit are 145.66 W and 14.71 W in order.
- The performance of the solar collector and cooking unit as well as the overall efficiencies of the indirect solar cooker increase by

Table 5
The comparison of the characteristics and performance of indirect solar cooker in the present study with those in previous researches.

Ref.	System mode	Heat transfer fluid	Using PCM	Cooking unit efficiency (%)		Solar cooker efficiency (%)	
				Energy	Exergy	Energy	Exergy
Present study	Single-stage/With pump	Oil	No	56.86	35.29	12.85	1.26
Present study	Single-stage/With pump	MWCNT-oil (0.2 wt%)	No	61.58	40.74	15.93	1.73
Present study	Single-stage/With pump	MWCNT-oil (0.5 wt%)	No	69.42	44.42	20.08	2.09
[7]	Single-stage/Thermosyphon	Water and refrigerants (R-22, R-134a, R-407C)	No	N/A	N/A	N/A	N/A
[10]	Double-stage/With pump	Therminol 55 oil	Yes (D-Mannitol)	41	N/A	9	N/A
[11]	Single-stage/Thermosyphon	Coconut oil	No	N/A	N/A	N/A	N/A
[12]	Single-stage/Thermosyphon	Oil	No	N/A	N/A	N/A	N/A
[13]	Single-stage/With pump	Water	Yes (Erythritol)	N/A	N/A	N/A	N/A
[14]	Single-stage/Thermosyphon	Oil	No	N/A	N/A	20–30	4–6
[16]	Double-stage/With pump	Therminol 55 oil	Yes (D-Mannitol)	73.5	N/A	10.2	N/A
[18]	Single-stage/Thermosyphon	Water and engine oil	Yes (Acetanilide)	N/A	N/A	N/A	N/A
[19]	Single-stage/Thermosyphon	Graphene-oil	No	N/A	N/A	N/A	N/A

rising the mass fraction of MWCNT nanoparticles. The overall energy efficiency of the solar cooker with thermal oil and the nanofluids with 0.2 wt% and 0.5 wt% is 12.85%, 15.93% and 20.08% respectively.

- The use of MWCNT-oil nanofluid with 0.5 wt% in preference to thermal oil reduces the time taken to boil 2 L of water about 23 min (31.51%).

According to the results, the use of MWCNT-oil nanofluid is an appropriate method to improve the performance of the indirect solar cooker from the energy and exergy viewpoints. Furthermore, PCM-based indirect solar cookers can provide the possibility of cooking in the evening or at night. Thus, future research can be focused on the effect of the simultaneous use of nanofluids and PCMs on the energy and exergy efficiencies of indirect solar cookers.

CRediT authorship contribution statement

Mohammad Hosseinzadeh: Methodology, Formal analysis, Data curation, Writing - original draft, Visualization. **Reza Sadeghirad:** Conceptualization, Methodology, Validation, Formal analysis, Investigation. **Hosein Zamani:** Conceptualization, Resources, Writing - review & editing, Supervision. **Ali Kianifar:** Methodology, Supervision. **Seyyed Mahdi Mirzababaee:** Data curation, Writing - review & editing.

Declaration of competing interest

The authors declare that they have no known competing financial interests or personal relationships that could have appeared to influence the work reported in this paper.

References

[1] A.N. Al-Shamani, M.H. Yazdi, M.A. Alghoul, A.M. Abed, M.H. Ruslan, S. Mat, K. Sopian, Nanofluids for improved efficiency in cooling solar collectors—a review, Renew. Sustain. Energy Rev. 38 (2014) 348–367.

[2] M. Hosseinzadeh, M. Sardarabadi, M. Passandideh-Fard, Energy and exergy analysis of nanofluid based photovoltaic thermal system integrated with phase change material, Energy 147 (2018) 636–647.

[3] A. Kazemian, M. Hosseinzadeh, M. Sardarabadi, M. Passandideh-Fard, Effect of glass cover and working fluid on the performance of photovoltaic thermal (PVT) system: an experimental study, Sol. Energy 173 (2018) 1002–1010.

[4] K. Chopra, A.K. Pathak, V.V. Tyagi, A.K. Pandey, S. Anand, A. Sari, Thermal performance of phase change material integrated heat pipe evacuated tube solar collector system: an experimental assessment, Energy Convers. Manag. 203 (2020), 112205.

[5] S.K. Verma, K. Sharma, N.K. Gupta, P. Soni, N. Upadhyay, Performance comparison of innovative spiral shaped solar collector design with conventional flat plate solar collector, Energy 194 (2020), 116853.

[6] M. Hosseinzadeh, A. Faezian, S.M. Mirzababaee, H. Zamani, Parametric analysis and optimization of a portable evacuated tube solar cooker, Energy 194 (2020) 116816.

[7] M. Esen, Thermal performance of a solar cooker integrated vacuum-tube collector with heat pipes containing different refrigerants, Sol. Energy 76 (6) (2004) 751–757.

[8] P. Stumpf, A. Balzar, W. Eisenmann, S. Wendt, H. Ackermann, K. Vajen, Comparative measurements and theoretical modelling of single-and double-stage heat pipe coupled solar cooking systems for high temperatures, Sol. Energy 71 (1) (2001) 1–10.

[9] S.Z. Farooqui, A vacuum tube based improved solar cooker, Sustain. Energy Technol. Assess. 3 (2013) 33–39.

[10] G. Kumaresan, R. Santosh, G. Raju, R. Velraj, Experimental and numerical investigation of solar flat plate cooking unit for domestic applications, Energy 157 (2018) 436–447.

[11] I. Haraksingh, I.A. Mc Doom, O.S.C. Headley, A natural convection flat-plate collector solar cooker with short term storage, Renew. Energy 9 (1–4) (1996) 729–732.

[12] K. Schwarzer, M.E.V. da Silva, Characterisation and design methods of solar cookers, Sol. Energy 82 (2) (2008) 157–163.

[13] S.D. Sharma, T. Iwata, H. Kitano, K. Sagara, Thermal performance of a solar cooker based on an evacuated tube solar collector with a PCM storage unit, Sol. Energy 78 (3) (2005) 416–426.

[14] S.Z. Farooqui, A review of vacuum tube based solar cookers with the experimental determination of energy and exergy efficiencies of a single vacuum tube based prototype, Renew. Sustain. Energy Rev. 31 (2014) 439–445.

[15] A. Mawire, M. McPherson, R.R.J. Van den Heetkamp, Simulated energy and exergy analyses of the charging of an oil–pebble bed thermal energy storage system for a solar cooker, Sol. Energy Mater. Sol. Cell. 92 (12) (2008) 1668–1676.

[16] G. Kumaresan, V.S. Vigneswaran, S. Esakkimuthu, R. Velraj, Performance assessment of a solar domestic cooking unit integrated with thermal energy storage system, J. Energy Storage 6 (2016) 70–79.

[17] R. Oommen, S. Jayaraman, Development and performance analysis of compound parabolic solar concentrators with reduced gap losses–oversized reflector, Energy Convers. Manag. 42 (11) (2001) 1379–1399.

[18] G. Saini, H. Singh, K. Saini, A. Yadav, Experimental investigation of the solar cooker during sunshine and off-sunshine hours using the thermal energy storage unit based on a parabolic trough collector, Int. J. Ambient Energy 37 (6) (2016) 597–608.

[19] M.S. Abd-Elhady, A.N.A. Abd-Elkerim, S.A. Ahmed, M.A. Halim, A. Abu-Oqal, Study the thermal performance of solar cookers by using metallic wires and nanographene, Renew. Energy 153 (2020) 108–116.

[20] R. Loni, E.A. Asli-Ardeh, B. Ghobadian, E. Bellos, W.G. Le Roux, Numerical comparison of a solar dish concentrator with different cavity receivers and working fluids, J. Clean. Prod. 198 (2018) 1013–1030.

[21] R. Loni, E.A. Asli-Ardeh, B. Ghobadian, A.B. Kasaeian, E. Bellos, Thermal performance comparison between Al_2O_3/oil and SiO_2/oil nanofluids in cylindrical cavity receiver based on experimental study, Renew. Energy 129 (2018) 652–665.

[22] A. Sarlak, A. Ahmadpour, M.R. Hajmohammadi, Thermal design improvement of a double-layered microchannel heat sink by using multi-walled carbon nanotube (MWCNT) nanofluids with non-Newtonian viscosity, Appl. Therm. Eng. 147 (2019) 205–215.

[23] A. Alirezaie, M.H. Hajmohammad, A. Alipour, M. salari, Do nanofluids affect the future of heat transfer?"A benchmark study on the efficiency of nanofluids", Energy 157 (2018) 979–989.

[24] R. Loni, E.A. Asli-Ardeh, B. Ghobadian, M.H. Ahmadi, E. Bellos, GMDH modeling and experimental investigation of thermal performance enhancement of hemispherical cavity receiver using MWCNT/oil nanofluid, Sol. Energy 171 (2018) 790–803.

[25] M. Hosseinzadeh, M. Sardarabadi, M. Passandideh-Fard, Nanofluid and phase change material integrated into a photovoltaic thermal system, in: V. Mittal (Ed.), Phase Change Materials, Central West Publishing, Australia, 2019, pp. 93–127.

[26] T.T. Chow, G. Pei, K.F. Fong, Z. Lin, A.L.S. Chan, J. Ji, Energy and exergy analysis of photovoltaic–thermal collector with and without glass cover, Appl. Energy 86 (3) (2009) 310–316.

[27] E. Cuce, Improving thermal power of a cylindrical solar cooker via novel micro/nano porous absorbers: a thermodynamic analysis with experimental validation, Sol. Energy 176 (2018) 211–219.

[28] N. Kumar, G. Vishwanath, A. Gupta, An exergy based test protocol for truncated pyramid type solar box cooker, Energy 36 (9) (2011) 5710–5715.

[29] A. Kumar, M. Sharma, P. Thakur, V.K. Thakur, S.S. Rahatekar, R. Kumar, A review on exergy analysis of solar parabolic collectors, Sol. Energy 197 (2020) 411–432.

[30] K. Wark, Advanced Thermodynamics for Engineers, McGraw-Hill, New York, 1995.

[31] M. González-Avilés, O.R. Urrieta, I. Ruiz, O.M. Cerutti, Design, manufacturing, thermal characterization of a solar cooker with compound parabolic concentrator and assessment of an integrated stove use monitoring mechanism, Energy Sustain. Develop. 45 (2018) 135–141.

[32] J. Yazdanpanahi, F. Sarhaddi, M.M. Adeli, Experimental investigation of exergy efficiency of a solar photovoltaic thermal (PVT) water collector based on exergy losses, Sol. Energy 118 (2015) 197–208.

[33] S. Pavlovic, R. Loni, E. Bellos, D. Vasiljević, G. Najafi, A. Kasaeian, Comparative study of spiral and conical cavity receivers for a solar dish collector, Energy Convers. Manag. 178 (2018) 111–122.

[34] H. Zamani, M. Moghiman, A. Kianifar, Optimization of the parabolic mirror position in a solar cooker using the response surface method (RSM), Renew. Energy 81 (2015) 753–759.

[35] M. Sardarabadi, M. Hosseinzadeh, A. Kazemian, M. Passandideh-Fard, Experimental investigation of the effects of using metal-oxides/water nanofluids on a photovoltaic thermal system (PVT) from energy and exergy viewpoints, Energy 138 (2017) 682–695.